Article

Performance Analysis of a 50 MW Solar PV Installation at BUI Power Authority: A Comparative Study between Sunny and Overcast Days

Rahimat Oyiza Yakubu [1,*], Muzan Williams Ijeoma [2,3,*], Hammed Yusuf [4], Abdulazeez Alhaji Abdulazeez [5], Peter Acheampong [6] and Michael Carbajales-Dale [2,3,*]

1   Department of Mechanical Engineering, Kwame Nkrumah University of Science and Technology, Kumasi AK-385-1973, Ghana
2   Department of Environmental Engineering and Earth Sciences, Clemson University, Clemson, SC 29634, USA
3   Energy, Economy and Environment (E3) Systems Analysis Group, Clemson University, Clemson, SC 29634, USA
4   Department of Mechanical Engineering Technology, Federal Polytechnic, Kama, Nasarawa 962101, Nigeria
5   Department of Chemical Engineering Technology, Federal Polytechnic, Kama, Nasarawa 962101, Nigeria
6   Bui Power Authority, BPA Heights, No 11 Dodi Link, Airport Residential Area, Accra GA-116-6933, Ghana
*   Correspondence: rahimayakubu@gmail.com (R.O.Y.); mijeoma@clemson.edu (M.W.I.); madale@clemson.edu (M.C.-D.)

Abstract: Ghana, being blessed with abundant solar resources, has strategically invested in solar photovoltaic (PV) technologies to diversify its energy mix and reduce the environmental impacts of traditional energy technologies. The 50 MW solar PV installation by the Bui Power Authority (BPA) exemplifies the nation's dedication to utilizing clean energy for sustainable growth. This study seeks to close the knowledge gap by providing a detailed analysis of the system's performance under different weather conditions, particularly on days with abundant sunshine and those with cloudy skies. The research consists of one year's worth of monitoring data for the climatic conditions at the facility and AC energy output fed into the grid. These data were used to analyze PV performance on each month's sunniest and cloudiest days. The goal is to aid in predicting the system's output over the next 365 days based on the system design and weather forecast and identify opportunities for system optimization to improve grid dependability. The results show that the total amount of AC energy output fed into the grid each month on the sunniest day varies between 229.3 MWh in December and 278.0 MWh in November, while the total amount of AC energy output fed into the grid each month on the cloudiest day varies between 16.1 MWh in August and 192.8 MWh in February. Also, the percentage variation in energy produced between the sunniest and cloudiest days within a month ranges from 16.9% (December) to 94.1% (August). The reference and system yield analyses showed that the PV plant has a high conversion efficiency of 91.3%; however, only the sunniest and overcast days had an efficiency of 38% and 92%, respectively. The BPA plant's performance can be enhanced by using this analysis to identify erratic power generation on sunny days and schedule timely maintenance to keep the plant's performance from deteriorating. Optimizing a solar PV system's design, installation, and operation can significantly improve its AC energy output, performance ratio, and capacity factor on sunny and cloudy days. The study reveals the necessity of hydropower backup during cloudy days, enabling BPA to calculate the required hydropower for a consistent grid supply. Being able to predict the daily output of the system allows BPA to optimize dispatch strategies and determine the most efficient mix of solar and hydropower. It also assists BPA in identifying areas of the solar facility that require optimization to improve grid reliability.

Keywords: solar PV system; solar radiation; AC energy output; performance ratio; system yield; capacity factor; solar PV performance analysis

1. Introduction

There is a growing global demand for sustainable energy solutions to reduce reliance on fossil fuels and decarbonize the energy supply sector, accelerating the adoption of renewable energy technologies and presenting a promising avenue for clean and renewable power generation [1,2]. Incorporating renewable energy sources such as solar, wind, hydro, geothermal, and biomass is essential to transitioning to sustainable and reliable energy systems. Hydroelectric power and solar photovoltaic (PV) systems stand out among renewable energy technologies as well-established technologies with the potential for significant environmental benefits [3–5]. However, the two technologies have limitations. PV systems are both variable and intermittent and cannot meet the power requirements alone throughout the year; hydropower generation is also variable depending on reservoir volume. Droughts or seasonal changes can dramatically reduce water availability and electricity production. Solar PV systems can operate during these dry spells to help meet energy demands [6,7]. Hybrid renewable energy systems, which combine multiple sources such as wind, solar, hydro, and other renewable energy resources, are increasingly being researched for their ability to provide a more stable and continuous power supply [8–10]. To improve the reliability of these two systems to supply steady power, we must be able to predict the system's output throughout the year based on the weather forecast. Comprehending the expected output will facilitate optimizing the system for improved performance [11,12].

Several studies have been conducted on hybrid systems worldwide. Cui et al. [13] discussed the hybridization of various ocean energy technologies, including wind, tidal currents, and geothermal energy. The authors proposed a system that combines multiple harvesting methods to boost energy production. Awan et al. [14] analyzed the performance of various hybrid systems. The renewable energy systems included solar + diesel + batteries, hydrogen storage + fuel cell(?), wind + diesel + fuel cells, solar + wind + diesel + pumped-hydro storage, and hydro + battery. Solar + wind + diesel + pumped-hydro storage achieved the highest renewable energy fraction (89.8%) and the most significant CO_2 emission reduction (89%) compared to diesel only. Aziz et al. [15] addressed the limitations of wind energy as a stand-alone technology. The research proposed combining wind with other backup systems, such as biomass or fuel cells, to create a more reliable hybrid system, making up for the intermittent wind resource. Khare et al. [16] examined the performance of a tidal + solar hybrid renewable energy system. They used various optimization techniques to assess the viability of the system in India. The simulation results show that a PV + tidal + battery + generator is the most economical solution for designing integrated systems compared to the PV, tidal, and battery.

In many other research articles, the synergy between solar PV and hydropower systems has been well documented. To reduce the operational load on hydro turbines, ensure steady power supply during low solar irradiance, and reduce operational and maintenance costs, Meshram et al. [7] proposed a system that combines 7.5 kW hydropower and 10 kW solar power. The system is linked to a utility grid. Converters were used to match the voltage of hydroelectric and solar systems to the grid voltage. Both hydroelectric and solar power plants use constant-current controllers. The results show that the proposed system can provide continuous power to consumers. Jurasz and Ciapała [17] presented a mathematical simulation and optimization model for achieving a hybrid solar-hydro system. Hydropower's flexibility complements solar variability, producing a more reliable and efficient renewable energy source. In the São Francisco River basin, where there have been severe droughts due to climate change, the integration of an optimized floating photovoltaic system (FPV) into a hydroelectric plant resulted in an average energy gain generated by the hydroelectric plant of 76%, with a capacity factor increase of 17.3% compared to six other hydroelectric plants. The PV system also contributes to lowering the levelized cost of electricity, depending on the geographical location of the FPV platform on the reservoir. The integration of FPV systems provides a dual benefit of renewable energy generation and water conservation [18].

Africa is widely regarded as the continent most affected by climate change [19,20]. This is despite Africa contributing the least to historic global greenhouse gas (GHG) emissions [21]. Climate change has caused erratic rainfall and droughts across most of Africa. This directly impacts the water flow in rivers that supply hydropower plants, resulting in lower electricity generation during dry spells [22,23]. With more than 600 million people in Africa without access to electricity [24], the overall trend indicates the need for a more diverse and resilient power generation system. African countries are capitalizing on their abundant sunshine to implement hybrid hydro-solar PV systems [25–27]. With its plentiful solar resources, Ghana has strategically invested in solar PV to diversify its energy portfolio and reduce the environmental impact of conventional energy systems.

Ghana's Bui Power Authority's (BPA) current electricity generation system represents a strategic combination of these two renewable energy technologies: a 400 MW hydroelectric plant and a 50 MW solar PV system. This hybrid setup aims to improve energy stability, optimize resource utilization, and contribute to the national grid while minimizing environmental impact [28,29]. The performance of solar PV systems is highly dependent on weather conditions, specifically solar irradiance, ambient temperature, and system design [30–33]. Performance variability has been a subject of significant research, and numerous studies have highlighted the variability in PV system output due to changing weather conditions. For instance, Gu et al. [34] demonstrated that solar irradiance and temperature significantly affect the efficiency and power output of PV systems. Nwoye et al. [35] observed correlations between the efficiency of a PV system, wind speed, and ambient temperature. According to Padmavathi and Arul [36], variations in solar irradiance, temperature, and system losses impact the performance of a 3 MW grid-connected PV plant in India. The performance ratio was found to be independent of solar irradiation but correlates with the temperature, according to the research conducted by Adar et al. [37]. In addition, Divya et al. [38] reported that solar PV electricity generation is dependent on solar radiation, module temperature, and system losses. Enrique et al. [4] reported an annual performance ratio and a capacity factor of 79.24% and 19.77%, respectively, for an annual insolation of 1976 kWh/m^2.

Previous performance analyses focused on a PV system's monthly or, more often, yearly output. The performance variability of a solar PV system comparing two extreme days (sunny and overcast) is yet to be evaluated. Detailed performance analysis on sunny and overcast days can provide a comprehensive understanding of the system's behavior, leading to more accurate predictions, optimization, reliability, financial planning, and better planning for energy production throughout the year by better connecting projected generation with weather forecasts.

This study examines the operational performance of Ghana's Bui Power Authority's 50 MW solar PV system on two separate days each month: one with maximum sunlight (most sunny days) and one with minimal sunlight (overcast days). The goal is to aid in predicting the system's output over the next 365 days based on the existing operational output data and weather forecast and identify opportunities for system optimization to improve grid dependability. By examining these opposing scenarios, the paper hopes to shed light on the performance metrics and dependability of the solar PV system in various weather conditions and offer practical recommendations for optimizing performance in diverse weather scenarios.

2. Materials and Methods

The methods and materials used in the analysis are explained in detail in this section. It details the examined solar PV systems, the technical parameters, and the performance-related indices.

2.1. Location and Photovoltaic Plant

In northwestern Ghana, along the Black Volta River, sits the Bui Dam with latitude-longitude 8.28, −2.24, as shown in Figure 1. This hydroelectric facility, comprising

four generating units, boasts a 404-megawatt (MW) capacity. Three of these units are powerful Francis turbines, each capable of generating 133.33 MW, while the remaining unit is a smaller 4 MW turbinette (compact hydro turbines) [39].
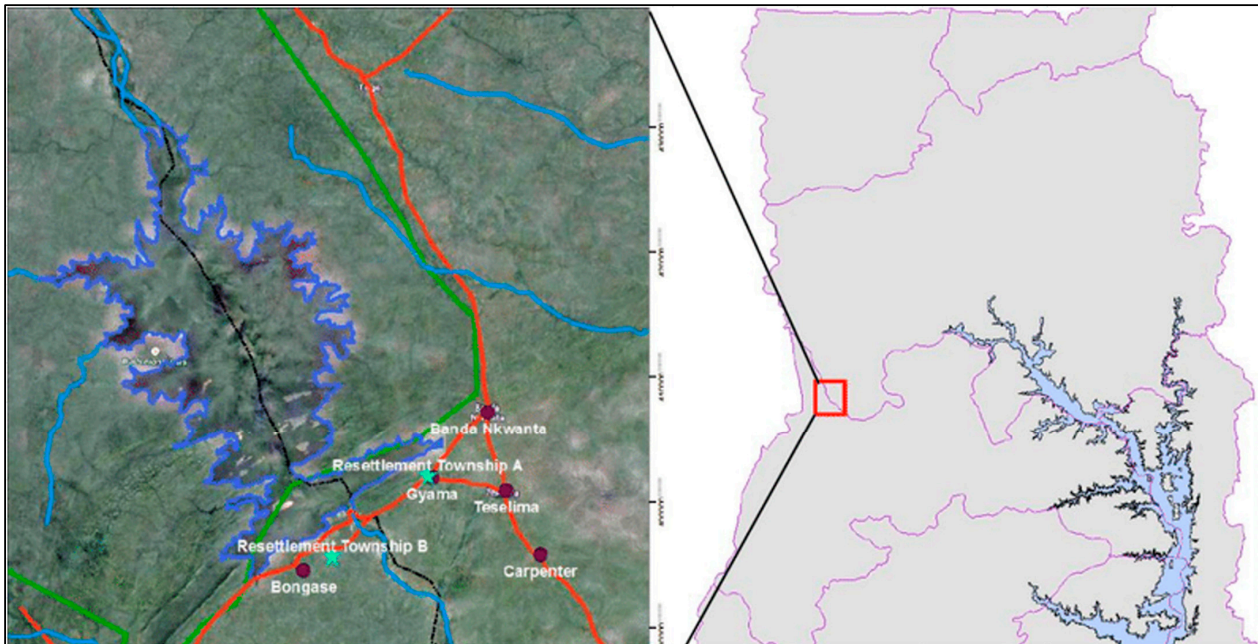

Figure 1. Location of Bui Hydro Dam (Source: OpenStreetMap latitude-longitude 8.28, −2.24) [40].

To boost the Bui dam's overall electricity generation without affecting the water reservoir, a 50-megawatt (MW) solar power plant was built on land 3 km from the dam, as shown in Figure 2. The solar plant was commissioned in November 2020. This solar PV plant uses monocrystalline PERC panels that capture sunlight only from the front and connect directly to the power grid.

Figure 2. The 50 MW solar PV plant at Bui (location: 8.26° N, 2.25° W).

2.2. Technical Design

The installed capacity of the grid-connected solar PV plant is 50.76 MWp. The solar plant's total net generating capacity is divided into sub-arrays of solar power capacity

that feed into power conditioning units (PCUs). The plant is a fixed-tilt ground-mounted system built downstream from the hydroelectric power plant. Table 1 shows the technical specifications of the PV system. The solar PV plant consists of 119,724 monocrystalline silicon modules. This project is connected to the grid at 34.5 kV and includes eight (8) transformers with capacities of 6.3 MVA each and 250 inverters. A single inverter has a capacity of 185 kW and 16/17/18 strings of 28/29/30 PV modules connected with capacities of 380 W/385 W/440 W [39].

Table 1. The 50 MW PV plant system parameters.

Parameter	Values
Location's geographical coordinates	8.26° N, 2.25° W
Maximum DC power capacity	50.768 MW
Inverter capacity	185 kW
Number of PV module	34,093/6480/79,016
PV module's power rating	380/385/440 Wp
Maximum AC power capacity	50 MW
Number of inverters	250
Number of PV modules per string	28/29/30
Maximum DC input voltage	34.5 kV
Number of strings per inverter	16/17/18
Transformer capacity	6.3 MVA
Number of Transformer	8
Ground clearance height	0.8–1.0 m
Tilt angle	5–8°
Orientation	South
DC/AC ratio	1.1

N stands for north, W stands for west, DC stands for direct current, AC stands for alternating current, MW stands for megawatt, Wp stands for watt peak, and kV stands for kilovolts.

Solar irradiance is crucial in evaluating solar PV systems, indicating the amount of power a surface receives per unit area. Solar irradiance comprises global horizontal irradiance (GHI), direct normal irradiance (DNI), and diffuse horizontal irradiance (DHI). DNI irradiance refers to the portion of solar irradiance directly reaching a surface. On the other hand, DHI is the portion scattered by the atmosphere. GHI is the combined diffuse and direct irradiance that reaches the same surface [41–43]. GHI and DHI represent a horizontal surface parallel to the ground, whereas DNI represents a perpendicular surface to the Sun. Higher values of the DHI/GHI ratio indicate an increased presence of clouds, greater air pollution, or higher levels of water vapor. GHI is strongly correlated with the Sun's location and, together with DNI, plays a crucial role in the functioning of solar systems. Practitioners utilize GHI forecasting, as stated by Law et al. [38], to evaluate the effectiveness of solar PV and thermal systems. Forecasting the use of both the GHI and DNI is crucial for assessing the performance of infrastructure in concentrating solar systems. Our system is a traditional solar PV system, so we considered the GHI values for the performance analysis.

The daily measured meteorological data consisting of GHI, ambient temperature, wind speed, sunshine time, power, and energy generated for the year 2022 were obtained from the Bui Power Authority (BPA). BPA has a meteorological station with a data logger stored on its server, which is monitored both physically and remotely. The instruments are calibrated yearly for accuracy. The server records the voltage, current, power factor, and power output of inverters for every minute. It also records solar irradiance, wind speed, and ambient temperature data from automatic weather stations.

The electric meter panel monitors and records this critical information. For the current study, the inverter monitoring system measured the hourly peak and average power and energy generated by EAC. The inverter measurements are sent to the supervisory control and data acquisition (SCADA) system installed in a high-performance workstation. The automatic generation control (AGC) and automatic voltage control (AVC) panels regulate

power generation and voltage levels to ensure grid stability and peak plant performance. Tracking energy production and consumption is essential for plant management. EAC stands for energy attribute certificate, usually issued for each megawatt-hour (MWh) of renewable electricity produced and added to the grid [44].

The International Energy Agency (IEA) developed performance parameters to analyze solar PV grid-interconnected systems. This study used reference yield, system yield, final yield, performance ratio, and capacity factor based on available data and literature [45]. It is important to note that when analyzing the system's output, Tanima et al. [46] stated that the ambient temperature should have a linear relationship with the PV module's output performance and efficiency.

2.3. Performance Related-Indices

The International Energy Agency (IEA) developed performance parameters to analyze solar PV grid-interconnected systems. Their study used reference yield, system yield, final yield, performance ratio, and capacity factor based on available data and literature [45]. These metrics are described below.

2.3.1. Reference Yield

The reference yield Y_r can be referred to as the ratio of daily total in-plane insolation (I_{POA}) to reference irradiance (G_{STC}) at standard test conditions (STC). It represents the available energy under ideal conditions. It is a function of the location, PV system design, and weather variability [4]. The equation is depicted as follows:

$$Y_{r,d} = \frac{I_{POA,\,d}}{G_{STC}} \left(\frac{\text{kWh}}{\text{kW-day}} \right) \tag{1}$$

2.3.2. System or Array Yield

Array yield (Ya) is the PV array's direct current (DC) energy output over a given period, normalized by the PV-rated power at STC. It represents the number of hours the PV array operates at its rated capacity. The Ya can be determined using:

$$Y_{a,d} = \frac{E_{DC}}{P_{PV,STC}} \left(\frac{\text{kWh}}{\text{kW-day}} \right) \tag{2}$$

The comparison between the system yield and the reference yield is a crucial set of performance parameters for a grid-connected solar system. This link represents the overall effectiveness of converting energy. The primary variables that require monitoring are the power transmitted to the electric grid and the level of irradiance within the plane. If the PV system is considered linear, then the system's output will be assumed to be directly linked to the reference output. The relationship between the measurements of system yield and reference yield can be estimated using a linear function that intersects the origin. The linear line can be determined by applying linear regression to all data samples. The slope of the line indicates the mean performance ratio across all data [45].

2.3.3. Final Yield

The final yield Y_f shows how close the actual electricity generated is to the ideal output. The final yield is calculated by dividing the total alternating current (AC) energy E_{AC} produced by the PV system over a specified period (a day, a month, or a year) by the installed PV array's peak power at a solar irradiance of 1000 W/m² and a cell temperature of 25 °C. This energy E_{AC} is the energy fed into the grid after inverter and transformer losses have been accounted for [47].

$$Y_{f,d} = \frac{E_{AC,d}}{P_{PV,STC}} \left(\frac{\text{kWh}}{\text{kW-day}} \right) \tag{3}$$

$$E_{AC,d} = \Sigma_{h=1}^{24} E_{AC,h} \,(\text{kWh}) \tag{4}$$

2.3.4. Performance Ratio (PR)

Performance ratio (PR) is the ratio of the energy injected into the grid to the nominal power of the installed PV array, i.e., the ratio of final yield to reference yield. It allows for comparison of performance results across different PV systems, regardless of geographical location or installed peak power [4,39]. The equation for the performance ratio is given as:

$$PR = \frac{Y_{f,d}}{Y_{r,d}} \times 100 \,(\%) \tag{5}$$

2.3.5. Capacity Factor

The capacity factor is a method of presenting the energy delivered by an electric power generation system. It is defined as the ratio of E_{AC}, the energy produced by the PV system over a given period to the energy output that would have been generated if the system had been operated at nominal capacity throughout the period [48]. The PV system's daily capacity factor is calculated using the following equation:

$$CF = \frac{E_{AC,d}}{P_{PV,STC} * 24} \times 100 \,(\%) \tag{6}$$

3. Results and Discussion

This section covers the results of the analysis based on the performance parameters and discusses them in the context of results from previous studies. These parameters include reference yield, system yield, final yield, performance ratio, and capacity factor.

3.1. Daily Solar Radiation Data Analysis

The meteorological and energy-generated data collected between January 2022 and December 2022 were analyzed to determine each month's most sunny and cloudy day. Figure 3 depicts the daily variation in solar radiation for each month's overcast and most sunny days. On cloudy days, the global horizontal irradiation (GHI) varies from 0.33 kWh/m^2 (August) to 4.02 kWh/m^2 (February), while sunny days experience a global horizontal irradiation ranging between 5.24 (September) and 6.94 kWh/m^2 (June). The graph shows that September has the lowest GHI, while June has the highest. This variability in solar radiation significantly affects the performance of a solar PV system. The GHI data indicate that, on sunny days, the system receives higher solar radiation, which is directly correlated with increased electricity generation. Conversely, on cloudy days, the reduced solar radiation results in lower energy production. The performance of a solar PV system is highly dependent on solar radiation and the ambient temperature [49,50]. This variability necessitates careful system design and sizing, potentially incorporating energy storage to balance supply [51]. To further elucidate the impact of weather conditions on system performance, a comparative analysis of energy generation on sunny and cloudy days was conducted. On average, sunny days produced approximately 50% more energy than cloudy days. This significant difference underscores the need for robust system design that can handle such fluctuations. For instance, in February, a sunny day with a GHI of 4.02 kWh/m^2 resulted in a 30% higher energy yield compared to an overcast day in the same month. This comparison highlights the critical role of solar radiation in determining the efficiency and productivity of solar PV systems.
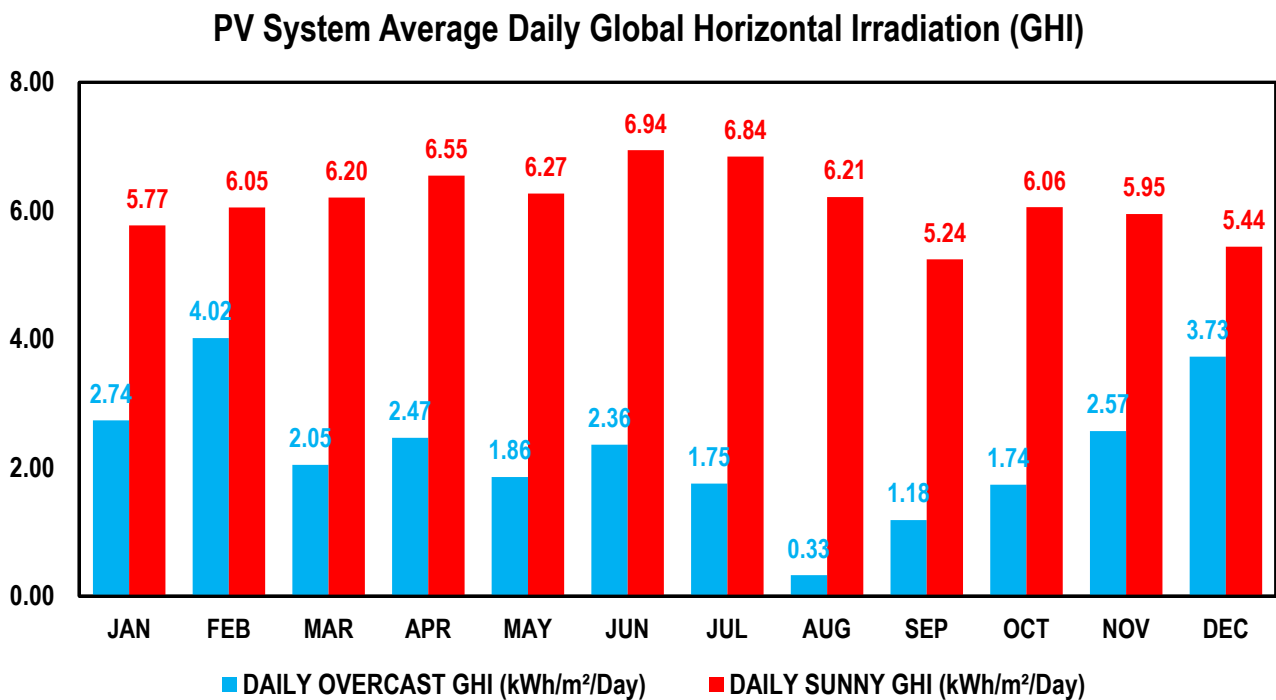
PV System Average Daily Global Horizontal Irradiation (GHI)

Figure 3. Average daily global horizontal irradiation of the solar PV system.

Figure 4(a1,a2),b,c depicts the relationship between the reference and system yields throughout the year, including the sunniest and cloudiest days. In Figure 4(a2),c, the reference and system yields are strongly correlated, indicating that the PV plant has a high conversion efficiency [45]. The coefficient of determination (R^2) is 0.913, indicating that the reference yield accounts for 91.3% of the total system yield throughout the year. On cloudy days (Figure 4c), the coefficient of determination is 0.927, demonstrating a strong predictive relationship. Sunny days, as depicted in Figure 4b, show less predictability between the reference yield and system yield, with a coefficient of determination of only 0.382. Solar PV systems tend to be less efficient at higher temperatures, which are more prevalent on sunny days [52]. This non-linear relationship between temperature and efficiency can cause variations that a linear regression model may not accurately capture. Furthermore, the performance of solar panels can degrade over time under intense sunlight due to overheating, leading to less predictable variations in output and a lower coefficient of determination [53]. These results align with the analytical grid-connected PV system performance study by Woyte et al. [45] in the IEA PVPS 2014 report, which found that module temperature is the most significant parameter affecting PV system performance. It could be seen that the sunny days are roughly constant throughout the year, whereas overcast days change with a roughly sinusoidal pattern throughout the year, so the lowest values are found during July–September. This study reinforces the importance of monitoring and managing the temperature to optimize the efficiency and output of solar PV systems. To address the lower predictability on sunny days, it is recommended that the BUI Power Authority consider implementing advanced cooling systems or selecting PV modules with better high-temperature performance characteristics. Additionally, regular maintenance and monitoring can help mitigate the effects of overheating and ensure consistent performance over time.
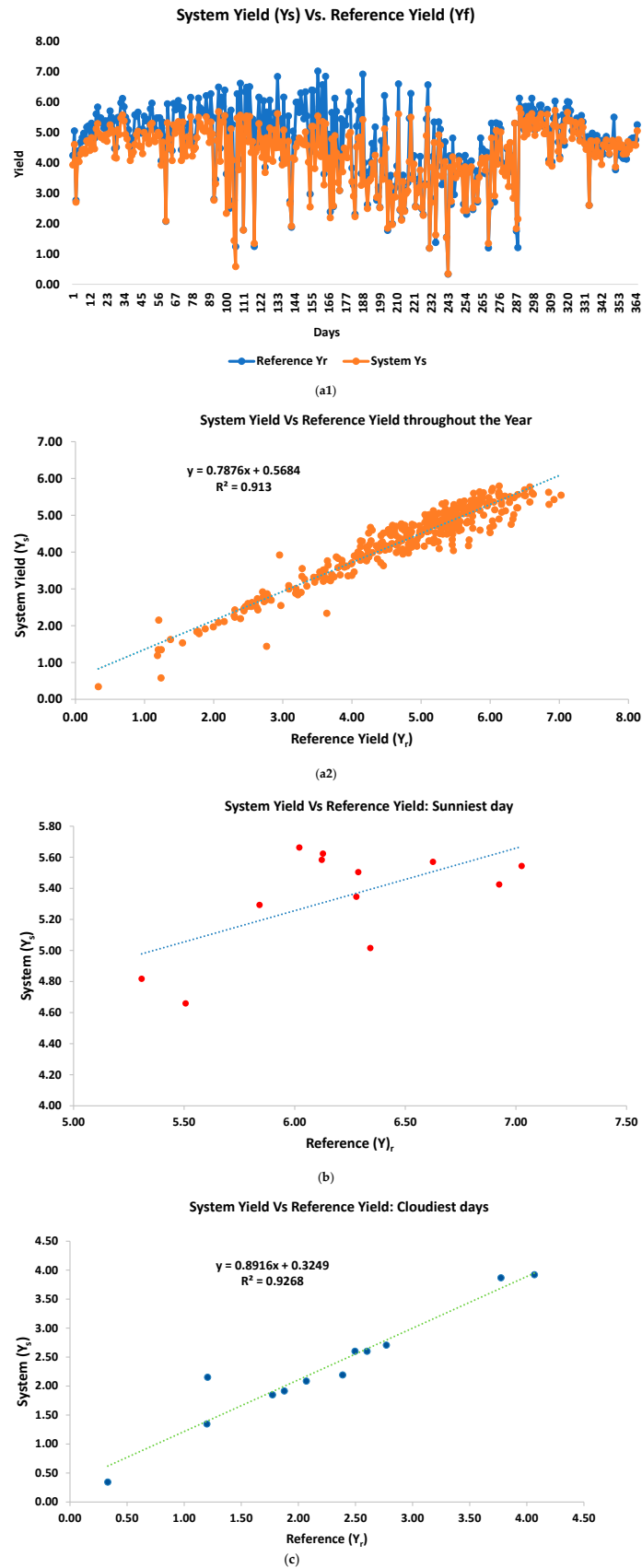
Figure 4. (**a1**) Daily system yield vs. reference yield: performance comparison throughout the year (365 days). (**a2**) Daily system yield versus reference yield throughout the year (365 days). (**b**) Daily system yield versus reference yield. (**c**) Daily system versus reference yield.

3.2. Daily Ambient Temperature and AC Energy Fed into the Grid (Sunny and Overcast Days)

Figure 5a,b shows the average ambient temperature and total AC energy generated per day on the most sunny and cloudy days of the year. The ambient temperature ranged from 22.6 °C (August) to 32.5 °C (February) during overcast days. On sunny days, the ambient temperature ranged from 27.1 °C (September) to 33.5 °C (February). It is worth noting that February has the highest average ambient temperature throughout the year, which makes it the hottest month for this location. The amount of AC energy fed into the grid on the sunniest day of the month varies between 229.3 MWh (December) and 278.0 MWh (November). Meanwhile, the cloudiest day of the month ranges between 16.1 MWh (August) and 192.8 MWh (February). A high energy output of 128.4 and 190.6 MWh was also observed in November and December. The percentage increase in energy generated on the sunniest day versus the cloudiest day ranges from 16.9% (December) to 94.1% (August). This significant variation underscores the correlation between total AC energy and available solar radiation. Increased irradiation directly leads to increased energy production, as seen in the higher energy outputs on sunny days. The analysis shows that the performance of the solar PV system is heavily influenced by seasonal variations in both solar radiation and ambient temperature. For instance, August, with the lowest average ambient temperature on overcast days, also shows the lowest energy output, emphasizing the combined impact of reduced solar radiation and lower temperatures on energy generation. February, characterized by the highest ambient temperatures, also exhibited substantial variations in energy output between sunny and cloudy days. The high ambient temperatures during this month likely contribute to thermal losses, which can decrease the efficiency of the PV system. This observation aligns with previous studies, indicating that solar PV systems are less efficient at higher temperatures due to increased thermal resistance in the PV modules.
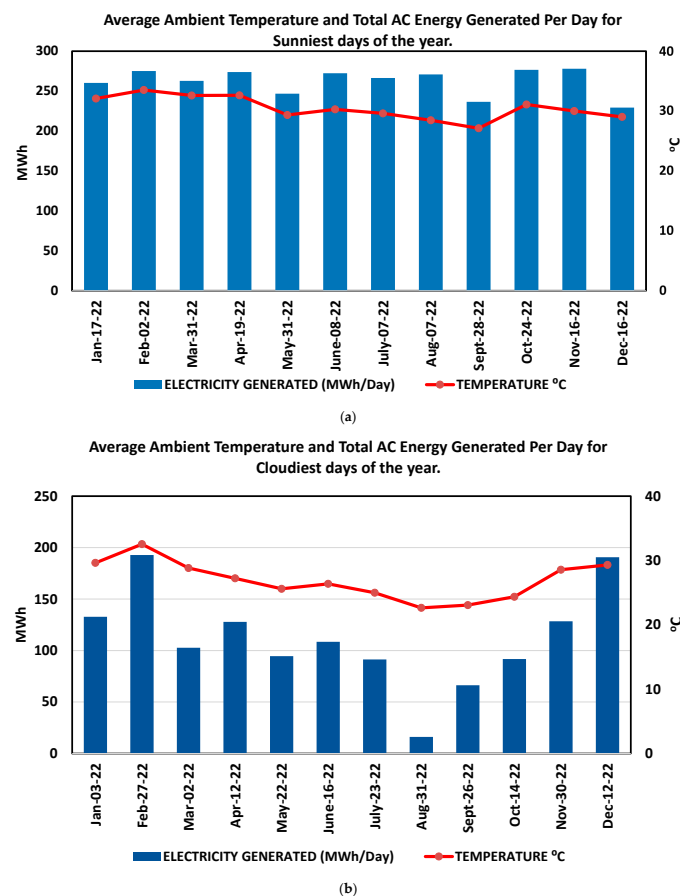

(a)

(b)

Figure 5. (**a**) The average ambient temperature and total AC energy generated per day on the Sunniest days of the year. (**b**) The average ambient temperature and total AC energy generated per day on the cloudiest (overcast) days of the year.

Nouar Aoun [49] reported a similar correlation between solar radiation and energy generated. The author conducted the energy and exergy analysis of a 20 MW grid-connected PV plant operating under harsh climate conditions in Southern Algeria for a period of 1 year. The author reported a monthly average daily ambient temperature minimum value of 14.05 °C in December and a maximum of 40.8 °C in July. The irradiation varied between 171.7 kWh/m^2 (January) and 251.2 kWh/m^2 (May). The total AC energy ranged between 2725.15 MWh (July) and 3447.5 MWh (March). The results show an agreement between the total AC energy and the total in-plane radiation; increasing the irradiation leads to increased total energy. However, the result of their study was based on a monthly average without a specific focus on cloudy and sunny days. It should be noted that the results reported by the Nouar Aoun study and this study agree that irradiation and ambient temperature significantly impact the value of energy generation. This also aligns with the conclusion made by Aoun N et al. [54], who evaluated the performance of monocrystalline PV modules under different weather and sky conditions and reported that irradiation and ambient temperature impact the value of energy generation.

3.3. Performance Ratio (PR)

The quality of the solar PV plant on these two contrasting days (sunniest and cloudiest) was examined by evaluating the performance ratio. A high-performance ratio indicates that the PV system efficiently converts available solar radiation to electrical energy [55]. As shown in Figure 6, the performance ratio of the solar PV system during the sunniest days fluctuates between 76.9 and 92.3%, while the performance ratio of the solar PV system for the overcast days is higher, ranging between 90.9 and 110.6%.
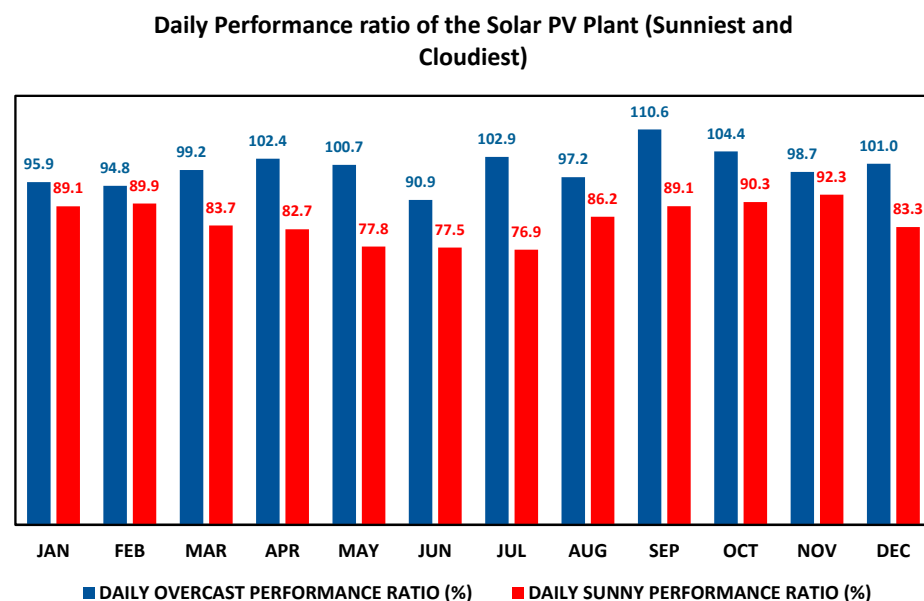

Daily Performance ratio of the Solar PV Plant (Sunniest and Cloudiest)

Figure 6. Daily performance ratio of the solar PV plant (sunniest and cloudiest).

According to the SMA Solar Technology AG technical report [56], while a performance ratio (PR) exceeding 100% for a solar PV system seems illogical, it can happen in certain circumstances, especially on cloudy days, due to the combined effects of diffuse light, cooler temperatures, and potential measurement anomalies. Also, depending on the installation location, plants and buildings can throw shadows on your PV plant's measuring gauge; hence, the measuring gauge can be temporarily or even permanently in the shade. Especially on cloudy days, parts of the PV plant can cast shadows over the measuring gauge. The partial or complete placement in the shadow of the measuring gauge can result in PR values of over 100%. The higher PR values on cloudy days, reaching up to 110.6%, highlight the complex interplay of environmental factors affecting the performance of solar

PV systems. While sunny days provide abundant solar radiation, the higher temperatures can reduce the overall efficiency, leading to lower PR values compared to cloudy days. Understanding these variations in PR is crucial for optimizing the design and operation of solar PV systems. The higher PR on cloudy days suggests that systems designed to maximize diffuse light capture and operate efficiently at lower temperatures can perform better under variable weather conditions.

The result of the PR of this study correlates with the PR reported by Fuster-Palop et al. and Mahadi et al. [4,51]. In their study, they both reported PRs of 75.2% and 79.24% for a 50 MW solar PV plant, respectively. Similarly, Kumar et al. [57] analyzed the theoretical and operational PR of an installed 10 MW grid-connected PV system in India and reported a PR that correlates to the PR stipulated in our study. In their analysis, they reported an operational average PR ratio of 85.1%, with the highest PR of 97.5% in December and the lowest PR of 73.9% in April. They concluded that system malfunction could have led to the variation in PR and that the plant operated nearer to the predicted energy generation using software.

3.4. Daily Capacity Factor of the Solar PV Plant (Sunniest and Cloudiest)

The capacity factor was used to calculate how much energy the solar PV plant produces on sunny and overcast days versus the maximum amount of energy it could theoretically produce if it operated at full capacity on that same day. As depicted in Figure 7, the capacity factor for overcast days ranged between 1.3% and 16.1%, whereas sunny days exhibited a higher capacity factor, ranging between 19.1% and 23.2%. The lower capacity factor on overcast days is attributed to reduced solar insolation, as climatic conditions such as rain, cloudy skies, and storms diminish the amount of solar radiation reaching the PV panels [47]. The significant disparity in capacity factor between sunny and overcast days underscores the influence of climatic conditions on the performance of the solar PV plant. Overcast days, characterized by lower solar radiation, result in reduced energy output, hence a lower capacity factor. On the other hand, sunny days with higher solar radiation led to increased energy production and a higher capacity factor. The variability in capacity factor due to changing weather conditions emphasizes the need for robust system design and operational strategies to maximize energy production.
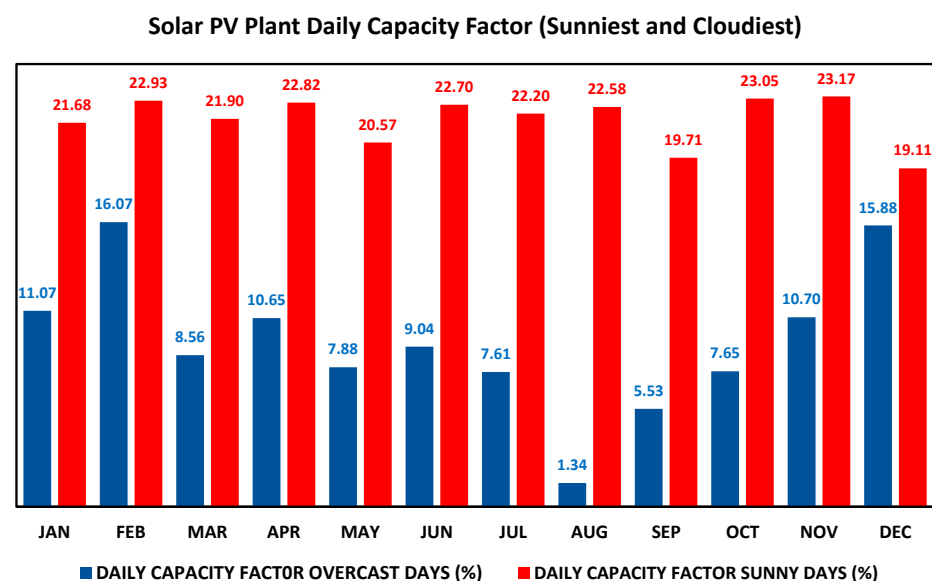

Figure 7. Daily capacity factor of the solar PV plant (sunniest and cloudiest).

4. Conclusions

The current study examines a 50 MW solar PV utility scale integrated with a hydropower plant owned by Ghana's Bui Power Authority (BPA). This article aims to add

to the growing knowledge of hybrid renewable energy systems by conducting a detailed performance analysis. By examining the system's output on the sunniest and most overcast days, the study provides valuable insights into operational dynamics and potential improvements for such seasonal variation. This analysis is critical for improving the integration and performance of renewable energy systems, thereby promoting sustainable energy development in Ghana and beyond.

The research consists of a one-year monitoring period with measurements of climatic data and AC energy output fed into the grid. Using these data, the PV performance was analyzed for each month's sunniest and most overcast days. The outcome of the research is summarized as follows: The amount of AC energy fed into the grid on the sunniest day of the month ranges from 229.3 MWh (December) to 278.0 MWh (November), and the cloudiest day of the month averages 16.1 MWh (August) and 192.8 MWh (February). The percentage increase in energy generated between the sunniest and cloudiest days ranges from 16.9% (December) to 94.1% (August). During the sunniest days, the solar PV system's performance ratio ranges from 76.9 to 92.3%, while on overcast days, it ranges from 90.9 to 110.6%. Finally, the capacity factor values for overcast days ranged from 1.34 to 16.07%, whereas sunny days had a higher capacity factor ranging from 19.11 to 23.17%.

This analysis of the BPA solar plant's performance on sunny and cloudy days helps the BPA optimize hydropower usage through Hydro Support; knowing how much solar power the plant produces on a sunny day enables BPA to use hydropower strategically. During peak solar hours, they may be able to reduce hydropower output, saving water in the reservoir for times when solar is limited. This analysis also shows that a hydro backup is needed during cloudy days, and our results provide information on the minimum solar power generation. BPA can use these data to calculate the amount of hydropower required to maintain a consistent grid supply during periods of low solar output. Finally, the result of this study helps BPA understand the solar plant's variability, enabling their ability to optimize dispatch strategies and determine the most efficient mix of solar and hydropower to deliver to the grid at various times.

Furthermore, epileptic power generation on a sunny day, compared to predictions, could signal trouble with solar panels or inverters. By catching these issues early with data analysis, maintenance can be done quickly to prevent the plant's performance from worsening. Implementing strategies such as optimizing the panel orientation and tilt, use of high-efficiency panels, power optimizers, appropriate ground cover ratio, ensuring proper cooling and regular maintenance, and optimal site locations can improve the AC energy output, performance ratio, and capacity factor of a solar PV system during both sunny and overcast days.

References

1. Kougias, I.; Szabó, S.; Monforti-Ferrario, F.; Huld, T.; Bódis, K. A methodology for optimization of the complementarity between small-hydropower plants and solar PV systems. *Renew. Energy* **2016**, *87*, 1023–1030. [CrossRef]
2. Syahputra, R.; Soesanti, I. Renewable energy systems based on micro-hydro and solar photovoltaic for rural areas: A case study in Yogyakarta, Indonesia. *Energy Rep.* **2021**, *7*, 472–490. [CrossRef]
3. Lee, N.; Grunwald, U.; Rosenlieb, E.; Mirletz, H.; Aznar, A.; Spencer, R.; Cox, S. Hybrid floating solar photovoltaics-hydropower systems: Benefits and global assessment of technical potential. *Renew. Energy* **2020**, *162*, 1415–1427. [CrossRef]
4. Fuster-Palop, E.; Vargas-Salgado, C.; Ferri-Revert, J.C.; Payá, J. Performance analysis and modelling of a 50 MW grid-connected photovoltaic plant in Spain after 12 years of operation. *Renew. Sustain. Energy Rev.* **2022**, *170*, 112968. [CrossRef]
5. Piancó, F.; Moraes, L.; Prazeres, I.D.; Lima, A.G.G.; Bessa, J.G.; Micheli, L.; Fernández, E.; Almonacid, F. Hydroelectric operation for hybridization with a floating photovoltaic plant: A case of study. *Renew. Energy* **2022**, *201*, 85–95. [CrossRef]
6. Farfan, J.; Breyer, C. Combining floating solar photovoltaic power plants and hydropower reservoirs: A virtual battery of great global potential. *Energy Procedia* **2018**, *155*, 403–411. [CrossRef]
7. Meshram, S.; Agnihotri, G.; Gupta, S. Performance analysis of grid integrated hydro and solar based hybrid systems. *Adv. Power Electron.* **2013**, *2013*, 697049. [CrossRef]
8. Stiubiener, U.; da Silva, T.C.; Trigoso, F.B.M.; da Silva Benedito, R.; Teixeira, J.C. PV power generation on hydro dam's reservoirs in Brazil: A way to improve operational flexibility. *Renew. Energy* **2020**, *150*, 765–776. [CrossRef]
9. Zhou, Y.; Chang, F.J.; Chang, L.C.; Lee, W.D.; Huang, A.; Xu, C.Y.; Guo, S. An advanced complementary scheme of floating photovoltaic and hydropower generation flourishing water-food-energy nexus synergies. *Appl. Energy* **2020**, *275*, 115389. [CrossRef]
10. Zhang, Y.; Ma, C.; Lian, J.; Pang, X.; Qiao, Y.; Chaima, E. Optimal photovoltaic capacity of large-scale hydro-photovoltaic complementary systems considering electricity delivery demand and reservoir characteristics. *Energy Convers. Manag.* **2019**, *195*, 597–608. [CrossRef]
11. Chi, L.; Su, H.; Zio, E.; Qadrdan, M.; Zhou, J.; Zhang, L.; Fan, L.; Yang, Z.; Xie, F.; Zuo, L.; et al. A systematic framework for the assessment of the reliability of energy supply in Integrated Energy Systems based on a quasi-steady-state model. *Energy* **2023**, *263*, 125740. [CrossRef]
12. Li, Z.; Wang, Z.; Fu, Y.; Zhao, N. Energy supply reliability assessment of the integrated energy system considering complementary and optimal operation during failure. *IET Gener. Transm. Distrib.* **2021**, *15*, 1897–1907. [CrossRef]
13. Cui, L.; Amani, S.; Gabr, M.; Kumari, W.G.; Ahmed, A.; Ozcan, H.; Horri, B.A.; Bhattacharya, S. Synergistic Hybrid Marine Renewable Energy Harvest System. *Energies* **2024**, *17*, 1240. [CrossRef]
14. Awan, A.B.; Zubair, M.; Sidhu, G.A.S.; Bhatti, A.R.; Abo-Khalil, A.G. Performance analysis of various hybrid renewable energy systems using battery, hydrogen, and pumped hydro-based storage units. *Int. J. Energy Res.* **2019**, *43*, 6296–6321. [CrossRef]
15. Aziz, M.S.; Ahmed, S.; Saleem, U.; Mufti, G.M. Wind-hybrid power generation systems using renewable energy sources—A review. *Int. J. Renew. Energy Res.* **2017**, *7*, 111–127. [CrossRef]
16. Khare, V. Prediction, investigation, and assessment of novel tidal–solar hybrid renewable energy system in India by different techniques. *Int. J. Sustain. Energy* **2019**, *38*, 447–468. [CrossRef]
17. Jurasz, J.; Ciapała, B. Solar–hydro hybrid power station as a way to smooth power output and increase water retention. *Solar Energy* **2018**, *173*, 675–690. [CrossRef]
18. Silvério, N.M.; Barros, R.M.; Tiago Filho, G.L.; Redón-Santafé, M.; dos Santos, I.F.S.; de Mello Valerio, V.E. Use of floating PV plants for coordinated operation with hydropower plants: Case study of the hydroelectric plants of the São Francisco River basin. *Energy Convers. Manag.* **2018**, *171*, 339–349. [CrossRef]
19. Adepoju, P. Africa Worst Hit by Climate Change Impacts, COP26 Told. Available online: https://www.nature.com/articles/d44148-021-00107-z (accessed on 6 June 2024).
20. United Nations Economic Commission for Africa. 17 out of the 20 Countries Most Threatened by Climate Change Are in Africa, But There Are Still Solutions to This Crisis. Available online: https://www.uneca.org/stories/17-out-of-the-20-countries-most-threatened-by-climate-change-are-in-africa,-but-there-are (accessed on 6 June 2024).
21. Weber, T.; Haensler, A.; Rechid, D.; Pfeifer, S.; Eggert, B.; Jacob, D. Analyzing Regional Climate Change in Africa in a 1.5, 2, and 3 °C Global Warming World. *Earths Future* **2018**, *6*, 643–655. [CrossRef]
22. Niang, I.; Ruppel, O.C. Africa. In *Climate Change 2014—Impacts, Adaptation and Vulnerability: Part B: Regional Aspects*; Cambridge University Press: Cambridge, UK; New York, NY, USA, 2014. [CrossRef]
23. Sissoko, K.; van Keulen, H.; Verhagen, J.; Tekken, V.; Battaglini, A. Agriculture, livelihoods and climate change in the West African Sahel. *Reg. Environ. Chang.* **2011**, *11* (Suppl. S1), 119–125. [CrossRef]
24. Ijeoma, M.W.; Lewis, C.G.; Chen, H.; Chukwu, B.N.; Carbajales-Dale, M. Technical, economic, and environmental feasibility assessment of solar-battery-generator hybrid energy systems: A case study in Nigeria. *Front. Energy Res.* **2024**, *12*, 1397037. [CrossRef]
25. IEA. Access to Electricity—SDG7: Data and Projections—Analysis—IEA. Available online: https://www.iea.org/reports/sdg7-data-and-projections/access-to-electricity (accessed on 4 April 2022).
26. Sanchez, R.G.; Kougias, I.; Moner-Girona, M.; Fahl, F.; Jäger-Waldau, A. Assessment of floating solar photovoltaics potential in existing hydropower reservoirs in Africa. *Renew. Energy* **2021**, *169*, 687–699. [CrossRef]

27. Energy Sector Management Assistance Program; Solar Energy Research Institute of Singapore. *Where Sun Meets Water*; World Bank: Washington, DC, USA, 2019. [CrossRef]

28. 2019 Energy Commission. *Ghana Renewable Energy Master Plan*; Energy Commission: Accra, Ghana, 2019; pp. 1–83.

29. GWÉNAËLLE DEBOUTTE. First Unit of 250 MW Floating PV Project Comes Online in Ghana—PV Magazine International. PV Magazine. Available online: https://www.pv-magazine.com/2020/12/15/first-unit-of-250-mw-floating-pv-project-comes-online-in-ghana/ (accessed on 1 January 2023).

30. Hasan, M. Design 50MW Large Scale PV Power Plant Considering Bangladeshi Climate. Ph.D. Thesis, Uppsala Universitet, Uppsala, Sweden, 2021.

31. Yakubu, R.O.; Mensah, L.D.; Quansah, D.A. Improving solar photovoltaic installation energy yield using bifacial modules and tracking systems: An analytical approach. *Adv. Mech. Eng.* **2022**, *14*, 16878132221139714. [CrossRef]

32. Yakubu, R.O.; Ankoh, M.T.; Mensah, L.D.; Quansah, D.A.; Adaramola, M.S. Predicting the Potential Energy Yield of Bifacial Solar PV Systems in Low-Latitude Region. *Energies* **2022**, *15*, 8510. [CrossRef]

33. Ijeoma, M.W.; Chen, H.; Carbajales-Dale, M.; Yakubu, R.O. Techno-Economic Assessment of the Viability of Commercial Solar PV System in Port Harcourt, Rivers State, Nigeria. *Energies* **2023**, *16*, 6803. [CrossRef]

34. Gu, W.; Ma, T.; Li, M.; Shen, L.; Zhang, Y. A coupled optical-electrical-thermal model of the bifacial photovoltaic module. *Appl. Energy* **2020**, *258*, 114075. [CrossRef]

35. Nwoye, C.I.; Emelue, H.U.; Bamidele, F.A.; Owadara, A.B. Empirical Analysis of Performance Efficiency of Monocrystalline Silicon Solar Photovoltaic Module Based on Ambient Temperature and Wind Speed. *Int. J. Phys.* **2020**, *1*, 1–5.

36. Padmavathi, K.; Daniel, S.A. Performance analysis of a 3 MWp grid connected solar photovoltaic power plant in India. *Energy Sustain. Dev.* **2013**, *17*, 615–625. [CrossRef]

37. Adar, M.; Najih, Y.; Gouskir, M.; Chebak, A.; Mabrouki, M.; Bennouna, A. Three PV plants performance analysis using the principal component analysis method. *Energy* **2020**, *207*, 118315. [CrossRef]

38. Mittal, D.; Saxena, B.K.; Rao, K.V.S. Comparison of floating photovoltaic plant with solar photovoltaic plant for energy generation at Jodhpur in India. In Proceedings of the 2017 IEEE International Conference on Technological Advancements in Power and Energy: Exploring Energy Solutions for an Intelligent Power Grid, TAP Energy 2017, Kollam, India, 21–23 December 2017; pp. 1–6. [CrossRef]

39. Yakubu, R.O.; Quansah, D.A.; Mensah, L.D.; Ahiataku-togobo, W.; Acheampong, P.; Adaramola, M.S. Comparison of ground-based and floating solar photovoltaic systems performance based on monofacial and bifacial modules in Ghana. *Energy Nexus* **2023**, *12*, 100245. [CrossRef]

40. Nominatim. Reverse Result for 8.27849,-2.23640. Available online: https://nominatim.openstreetmap.org/ui/reverse.html?lat=8.27849&lon=-2.23640&zoom=18 (accessed on 10 August 2024).

41. Lujano-Rojas, J.; Dufo-López, R.; Domínguez-Navarro, J.A. Forecasting of electricity prices, demand, and renewable resources. In *Genetic Optimization Techniques for Sizing and Management of Modern Power Systems*; Elsevier: Amsterdam, The Netherlands, 2023; pp. 201–246. [CrossRef]

42. Law, E.W.; Prasad, A.A.; Kay, M.; Taylor, R.A. Direct normal irradiance forecasting and its application to concentrated solar thermal output forecasting—A review. *Solar Energy* **2014**, *108*, 287–307. [CrossRef]

43. Intergovernmental Panel on Climate Change. *Climate Change*; Cambridge University Press: Cambridge, UK, 2007; Available online: https://assets.cambridge.org/97805217/05967/frontmatter/9780521705967_frontmatter.pdf (accessed on 6 June 2024).

44. US EPA. Energy Attribute Certificates (EACs). Available online: https://www.epa.gov/green-power-markets/energy-attribute-certificates-eacs (accessed on 6 June 2024).

45. Woyte, A.; Richter, M.; Moser, D.; Reich, N.; Green, M.; Mau, S.; Beyer, H.G. *Analytical Monitoring of Grid-Connected Photovoltaic Systems Good Practices for Monitoring and Performance Analysis: IEA PVPS Task 13, Subtask 2: Report IEA PVPS T13-03: 2014*; International Energy Agency Photovoltaic Power Systems Program: Paris, France, 2014.

46. Bhattacharya, T.; Chakraborty, A.K.; Pal, K. Effects of Ambient Temperature and Wind Speed on Performance of Monocrystalline Solar Photovoltaic Module in Tripura, India. *J. Sol. Energy* **2014**, *2014*, 817078. [CrossRef]

47. Veerendra Kumar, D.J.; Deville, L.; Ritter, K.A., III; Raush, J.R.; Ferdowsi, F.; Gottumukkala, R.; Chambers, T.L. Performance Evaluation of 1.1 MW Grid-Connected Solar Photovoltaic Power Plant in Louisiana. *Energies* **2022**, *15*, 3420. [CrossRef]

48. Bolinger, M.; Seel, J.; Wu, M. Maximizing MWh: A statistical analysis of the performance of utility-scale photovoltaic projects in the United States. In Proceedings of the 2017 IEEE 44th Photovoltaic Specialist Conference, PVSC 2017, Washington, DC, USA, 25–30 June 2017; pp. 467–471. [CrossRef]

49. Aoun, N. Energy and exergy analysis of a 20-MW grid-connected PV plant operating under harsh climatic conditions. *Clean Energy* **2024**, *8*, 281–296. [CrossRef]

50. Meyer, E.L.; Buma, C.L.; Taziwa, R.T. Performance parameters of an off-grid building integrated photovoltaic system in South Africa. In Proceedings of the 33rd European Photovoltaic Solar Energy Conference and Exhibition, Amsterdam, The Netherlands, 25–29 September 2017; pp. 2450–2455.

51. Al Mehadi, A.; Nahin-Al-Khurram; Shagor, M.R.K.; Sarder, M.A.I. Optimized seasonal performance analysis and integrated operation of 50MW floating solar photovoltaic system with Kaptai hydroelectric power plant: A case study. *Energy Sources Part A Recovery Util. Environ. Eff.* **2021**, 1–25. [CrossRef]

52. Dhimish, M. Thermal impact on the performance ratio of photovoltaic systems: A case study of 8000 photovoltaic installations. *Case Stud. Therm. Eng.* **2020**, *21*, 100693. [CrossRef]

53. Dubey, S.; Sarvaiya, J.N.; Seshadri, B. Temperature dependent photovoltaic (PV) efficiency and its effect on PV production in the world—A review. *Energy Procedia* **2013**, *33*, 311–321. [CrossRef]

54. Aoun, N.; Bouchouicha, K.; Chenni, R. Performance Evaluation of a Mono-Crystalline Photovoltaic Module under Different Weather and Sky Conditions. *Int. J. Renew. Energy Res.* **2017**, *7*, 292–297.

55. Supapo, K.R.M.; Lozano, L.; Querikiol, E.M. Performance Evaluation of an Existing Renewable Energy System at Gilutongan Island, Cebu, Philippines. *J. Eng.* **2024**, *2024*, 3131377. [CrossRef]

56. SMA Solar Technology AG. Performance ratio-Quality factor for the PV plant. *Energy Syst.* **2016**, 1–9.

57. Kumar, B.S.; Sudhakar, K. Performance evaluation of 10 MW grid connected solar photovoltaic power plant in India. *Energy Rep.* **2015**, *1*, 184–192. [CrossRef]